

Protein Removal from Natural Rubber Latex with Fe₃O₄@Al₂O₃ Nanoparticle

I P. Mahendra,^{a,b} Mai K. Linh,^{b,c} Nguyen N. Thang,^{b,d} Vu T. Thuy,^b Le T. Trang,^{b,e}
Le X. Thinh,^{b,e} Nguyen T. H. Phuong,^b Nguyen T. Ha,^{b,e} Nghiem T. Thuong,^{b,e}
Seiichi Kawahara,^f Yoshimasa Yamamoto^g and Phan T. Nghia^{*,b,e}

^aDepartment of Chemistry, Faculty of Mathematics and Natural Sciences,
Universitas Sumatera Utara, 20155 Sumatera Utara, Indonesia

^bCenter for Rubber Science and Technology, Hanoi University of Science and Technology,
10000 Hanoi, Vietnam

^cVinacontrol Corporation Group, 10000 Hanoi, Vietnam

^dDepartment of Textile Material and Chemical Processing, School of Textile-Leather and Fashion,
Hanoi University of Science and Technology, 10000 Hanoi, Vietnam

^eSchool of Chemical Engineering, Hanoi University of Science and Technology, 10000 Hanoi, Vietnam

^fDepartment of Materials Science and Technology, Faculty of Engineering,
Nagaoka University of Technology, 940-2188 Nagaoka, Niigata, Japan

^gDepartment of Materials Science and Engineering, National Institute of Technology, Tokyo College,
1220-2 Kunugida-machi, 193-0997 Hachioji, Tokyo, Japan

The presence of protein in the natural rubber latex for the medical device manufacture seems to be the most considered compound due to its allergic effect. Magnetic coated alumina (Fe₃O₄@Al₂O₃) has been known as an adsorbent for organic substrates due to its performance through physical and/or chemical interaction. In the current study, we tried to figure out the potential of Fe₃O₄@Al₂O₃ to prepare low protein's natural rubber latex with and without the presence of surfactant through a continuous batch system. The dry rubber content, surfactant amount, and time during the incubation were investigated to determine the effective protein removal natural rubber. The highly deproteinized natural rubber was confirmed using Kjeldahl method, proven that the utilization of Fe₃O₄@Al₂O₃ could reduce the protein content from 0.38 to 0.016% in an optimum condition (dry rubber content of 10.00%; surfactant of 0.25%; Fe₃O₄@Al₂O₃ of 1.00 wt.%; and 15 min of incubation time). These results showed that Fe₃O₄@Al₂O₃ is a very good material to remove protein from natural rubber latex and this method can be performed using a continuous batch system.

Keywords: natural rubber, latex, protein removal, nanoparticle, Fe₃O₄@Al₂O₃

Introduction

Natural rubber (*Hevea brasiliensis*) latex contains various components from macromolecules to inorganic molecules. The commonly found macromolecules in the natural rubber latex are protein, lipid, and carbohydrate at 2.0, 1.3, and 1.5%, of dry weight, respectively.^{1,2} Many studies^{1,3-7} have tried to separate those impurities from the natural rubber latex. Protein is one of the unwanted contaminants in the natural rubber latex-based product

due to its allergic effect. Several studies^{2,8} reported the presence of protein, especially Hev b1, in the natural rubber latex which can cause allergic reaction to many individuals. Several methods^{1,3-8} have been developed to reduce the amount of the protein from natural rubber latex. The methods usually incorporated sodium dodecyl sulfate (SDS) in the deproteinization method as the surfactant binds the impurities or the proteins. Other method used a combination of urea and SDS, which resulted in a more significant result. Starting from the urea method, researchers have tried to modify or replace this chemical with alternatives, e.g., protease and acetone.

*e-mail: nghia.phantrung@hust.edu.vn

The modification of urea method by adding protease and acetone showed an outstanding result.⁹ All methods which used SDS, urea, modified urea + protease, modified urea + acetone, required batches process and long incubation time. Hence, this process is considered not suitable for the advancing world which need a rapid, effective, and efficient process.

The protein removal process from natural rubber latex can cause a dilemma due to the significant change on the physical, chemical, and mechanical properties after the treatments. As reported by Nun-anan *et al.*,¹⁰ the presence of nonrubber components naturally help the unvulcanized natural rubber through its green strength properties. The significant result after the chemical treatment using alkaline-acetone extraction showed that the unvulcanized natural rubber had poor elasticity, mechanical, rheological, and dynamic properties. The decrease on those properties were also found in three vulcanized natural rubber products with different protein content.¹¹ The agglomeration was observed after the addition of carbon black as the filler in the chemically treated natural rubber which has low protein content. The presence of protein and other nonrubber molecules are the main components that control the mechanical properties, processability and cure properties. However, this issue was only found when the natural rubber latex was treated with harsh chemicals, i.e., chlorine-based chemicals, alkaline solution, etc. In a patent document,¹² the properties of natural rubber latex that was treated using anionic-cationic interaction showed insignificant change with the untreated one.

Due to the advantages of the anionic-cationic interaction in the protein removal from natural rubber latex, in this current study we tried to evaluate the potential of magnetic nanoparticle that was assisted by anionic surfactant to reduce the protein content of natural rubber latex. Magnetic nanoparticle has been investigated comprehensively over the last decade and it was increasingly developed. As soft material, the separation of magnetic nanoparticles when used as adsorbent can be done by using external magnetic sources.^{13,14} The most common magnetic materials are based on iron oxides, due to the presence of large quantity of active site on its surface and enormous specific surface area.¹⁵ The other advantages are low toxicity and ease of dispersion in many matrixes. As a superparamagnetic material, the magnetic iron oxide is mostly found as an aggregate. To prevent aggregation, several techniques can be applied to overcome limitations, one of which by coating the surface of magnetic iron oxide using polymer or inorganic materials. This coating process has been proven to improve the chemical stability of magnetic iron oxide. In several studies,^{16,20} magnetic iron oxide has

been coated using gold, titan, alumina, and silica. Those inorganic materials will act as shells, while the magnetic iron oxide will act as the core. Among those materials, Al_2O_3 is the most ideal coating medium for the magnetic materials; in fact, this material features high chemical stability, bioinertness, and low susceptibility to hydrolysis and is easy to functionalize by wet chemical methods. By suitable coating, the magnetic dipole-dipole attractions among nanoparticles might be covered which could result in minimizing or preventing aggregation.²¹ The previous studies^{18,19,22} have shown the effectiveness of Fe_3O_4 coated Al_2O_3 ($\text{Fe}_3\text{O}_4@ \text{Al}_2\text{O}_3$) as adsorbent for immobilizing proteins, e.g., ovalbumin, heme and phosphoprotein.

We assumed this coated magnetic nanoparticle would be able to reduce the amount of protein in high ammonia natural rubber (HANR) latex through anionic-cationic interaction and hydrophobic interaction. The anionic-cationic interaction can be found between Al_2O_3 which has negative charge in $\text{pH} > 7$ and protein in the HANR solution; and the other protein can interact directly with the SDS that was added into the system. This mechanism process has been stated in several studies^{18,19,23} that used coated magnetic as an adsorbent for several types of protein. Furthermore, the presence of SDS in the system can interact with the Al_2O_3 surface and protein through hydrophobic interaction.²⁴ The hydrophobic interaction of SDS can be explained as the interaction of carbon chain of dodecyl with the carbon backbone of protein. The interaction of protein in the HANR with the surface of Al_2O_3 also can be explained as the hydrophobic interaction.²⁵⁻²⁷

The objective of this study was to evaluate the performance of $\text{Fe}_3\text{O}_4@ \text{Al}_2\text{O}_3$ nanoparticle in the protein removal of natural rubber compared to the methods that use urea-SDS, and SDS- $\text{Fe}_3\text{O}_4@ \text{Al}_2\text{O}_3$ nanoparticle. The effectiveness of SDS- $\text{Fe}_3\text{O}_4@ \text{Al}_2\text{O}_3$ in the deproteinization process was evaluated under several parameters, i.e., various dry rubber content, SDS concentration, and incubation time.

Experimental

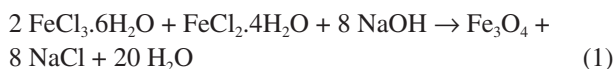
Materials

High ammonia natural rubber latex (HANR, dry rubber content = 60%) was obtained from the Dau Tieng Rubber Company, Vietnam Rubber Group (Vietnam). Sodium dodecyl sulfate was purchased from Fisher Scientific UK Ltd (United Kingdom). Urea was obtained from Nacalai Tesque, Inc (Japan). $\text{FeCl}_3 \cdot 6\text{H}_2\text{O}$ and $\text{FeCl}_2 \cdot 4\text{H}_2\text{O}$ were obtained from Merck (Singapore). All chemicals were used as received without further purification.

The synthesis of Fe₃O₄@Al₂O₃ nanoparticle

The synthesis of Fe₃O₄@Al₂O₃ nanoparticle was processed through two steps, i.e., preparation of magnetic iron oxide nanoparticle using co-precipitation, and coating process of alumina on the surface of magnetic iron oxide nanoparticle. Nanoparticle of Fe₃O₄@Al₂O₃ was prepared using the combination of previous methods.^{18,19,28}

Magnetic iron oxide nanoparticle was prepared according to the stoichiometric reaction:



Briefly, FeCl₃·6H₂O (0.0192 mol) and FeCl₂·4H₂O (0.0101 mol) were dissolved in 25 mL distilled water, sodium hydroxide (0.0102 mol) was added into the solution and the reaction was set at 80 °C for 30 min while being stirred at 500 rpm. The reaction was performed under nitrogenous atmosphere (5 mL min⁻¹). The obtained Fe₃O₄ was collected using magnet bar, followed by rinsing with deionized water until the pH reached 7.0. Approximately 65 mL of Al(NO₃)₃ 1.0 M solution was added into the 3-necks round bottom flask containing 100 mL magnetic iron oxide nanoparticle. The solution's pH was adjusted to 8 and the reaction was performed at 80 °C for 2 h and stirred at 500 rpm, the reaction was performed under nitrogenous atmosphere. The Fe₃O₄@Al(OH)₃ was rinsed using deionized water until the pH reached 7-8. The coating process was repeated to generate a double-layer Al(OH)₃ coating on the surface of Fe₃O₄ (Fe₃O₄@2Al(OH)₃) (Figure 1a). The yellowish-orange powder was obtained after calcination of double-layer Al(OH)₃ at 500 °C for 3 h. The as-prepared Fe₃O₄@Al₂O₃ (Figure 1b) was then

characterized using scanning electron microscopy (SEM, JEOL JSM-7600F), transmission electron microscopy (TEM, JEOL JEM-1010), and thermogravimetric analysis (TGA, NETZSCH STA 409 PC/PG).

Deproteinization of natural rubber latex

The HANR latex was diluted using distilled water until the dry rubber content of rubber was ± 10.00%. About 0.1 wt.% of SDS was added into the diluted HANR and stirred for 15 min. The pH of HANR solution was adjusted to 11 using 5.0% NH₄OH. Approximately 1.0 wt.% of the as-prepared Fe₃O₄@Al₂O₃ was added into the HANR solution and stirred for 30 min at 10 rpm. At the end of deproteinization, the Fe₃O₄@Al₂O₃-protein was collected using magnet bar. The yielded white solution or deproteinized natural rubber (DPNR) which has low protein content, was then filtered to remove impurities, and dried at 50 °C until reaching the constant weight. The described method above was repeated with different value of SDS content (0.05-0.25 wt.%), incubation time (15-75 min), and dry rubber content (5-25%). As the control, HANR was deproteinized using urea-SDS method. The nitrogen content of HANR and the obtained DPNR were determined using Kjeldahl method following a procedure from Rubber Research Institute of Malaysia.²⁹

The functional groups of HANR and DPNR were analyzed using Frontier IR/NIR FTIR (PerkinElmer), the samples were scanned 64 times with the spectra transmittance region between a wavenumber of 4000-500 cm⁻¹. The glass transition temperature of HANR and DPNR was determine using NETZSSCH STA 409 PC/PG. Samples were heated at rate of 10 °C min⁻¹ under an inert atmosphere of N₂ between -80 and 40 °C.

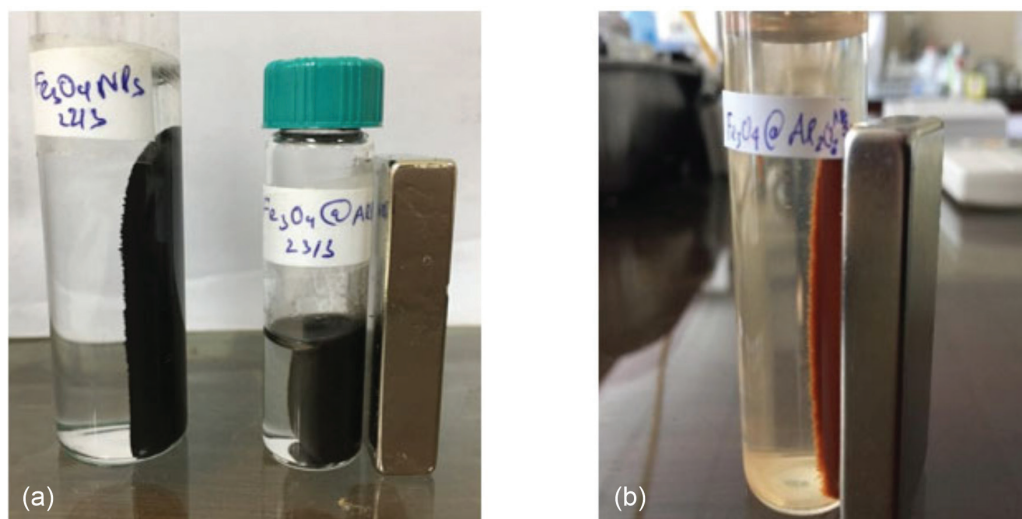


Figure 1. Fe₃O₄@2Al(OH)₃ (a) and Fe₃O₄@Al₂O₃ (b).

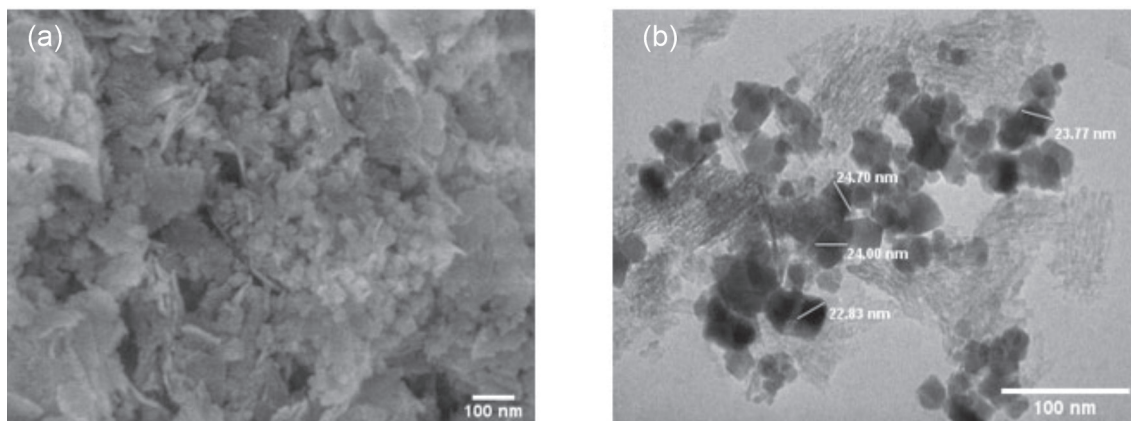


Figure 2. SEM image of $\text{Fe}_3\text{O}_4@Al_2O_3$ nanoparticle (a) and TEM image of $\text{Fe}_3\text{O}_4@Al_2O_3$ nanoparticle (b).

Results and Discussion

Characteristic of $\text{Fe}_3\text{O}_4@Al_2O_3$

The morphological analysis of $\text{Fe}_3\text{O}_4@Al_2O_3$ was visualized using SEM and TEM (Figures 2a and 2b). The visualization was performed to determine the morphology, particle size and shape of the as-prepared $\text{Fe}_3\text{O}_4@Al_2O_3$.

As can be seen in Figures 2a and 2b, the as-prepared $\text{Fe}_3\text{O}_4@Al_2O_3$ was in the range of nano-sized particle. Particle size analysis using ImageJ Fiji version³⁰ showed that the as-prepared $\text{Fe}_3\text{O}_4@Al_2O_3$ had an average particle size of 19.80 nm, at the range of 16-28 nm. The wide range of $\text{Fe}_3\text{O}_4@Al_2O_3$ particle size can be assumed as the consequence of the disruption of crystalline structure resulted from the impact of introducing alumina oxide into the magnetic iron oxide nanoparticle. The SEM image revealed that $\text{Fe}_3\text{O}_4@Al_2O_3$ nanoparticle consisted of irregular shapes (rods, squares, and small spheres) and has porous structure (large external pores, > 50 nm), a typical characteristic of alumina compound. The previous studies³¹⁻³³ revealed that $\text{Fe}_3\text{O}_4@Al_2O_3$ exist in various shapes, i.e., irregular, cubic, and hexagonal shape. The irregularly shaped $\text{Fe}_3\text{O}_4@Al_2O_3$ nanoparticle possess many advantageous, one of which is the presence of multiple sites for supporting the adsorption process, yet having a higher adsorption capacity.³¹ The TEM images revealed the shape of $\text{Fe}_3\text{O}_4@Al_2O_3$ nanoparticle as an aggregate and it showed the core and shell. The nanoparticle was constructed by magnetic iron oxide as the cores (black color) and the coating layer was constructed by alumina (grey color). By using ImageJ Fiji version,³⁰ the thickness of alumina can be estimated in range of 5-15 nm.

The thermal stability of $\text{Fe}_3\text{O}_4@Al_2O_3$ nanoparticle had been determined using TGA (Figure 3). The TGA graph showed mass loss of sample with increase temperature.

However, this analysis will have different results for different materials, especially due to the material composition.

Figure 3 (TGA curve, black line) showed four major loss regions, supported by the resulting DTG graph (Figure 3, blue line) of four peaks decomposition. The first peak can be called as initial mass loss, occurred at 7-138 °C, indicated the evaporation of the physisorbed water that was obtained from the environment.³² The second and third peaks that appeared at 224-295 and 333-483 °C corresponded to the dehydroxylation and dehydration, in which the dehydroxylation occurred due to the breaking of Al-OH bonds.^{32,34,35} Meanwhile, a minor mass loss can be found between 641-853 °C that was described as phase transformation of alumina and magnetic iron oxide nanoparticle from amorphous into crystalline with 76.10% of residual mass. The previous study³² mentioned that thermal stability of $\text{Fe}_3\text{O}_4@Al_2O_3$ can be enhanced by increasing the amount of Fe_3O_4 . It is obvious due to the presence of crystalline phase in Fe_3O_4 nanoparticle.

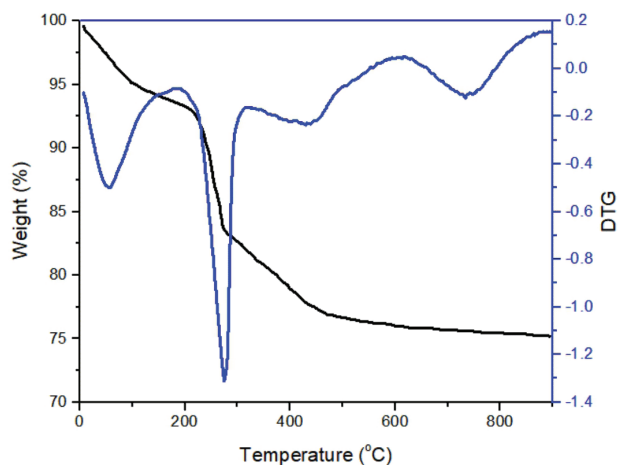


Figure 3. TGA and derivative thermogravimetric (DTG) curves of $\text{Fe}_3\text{O}_4@Al_2O_3$.

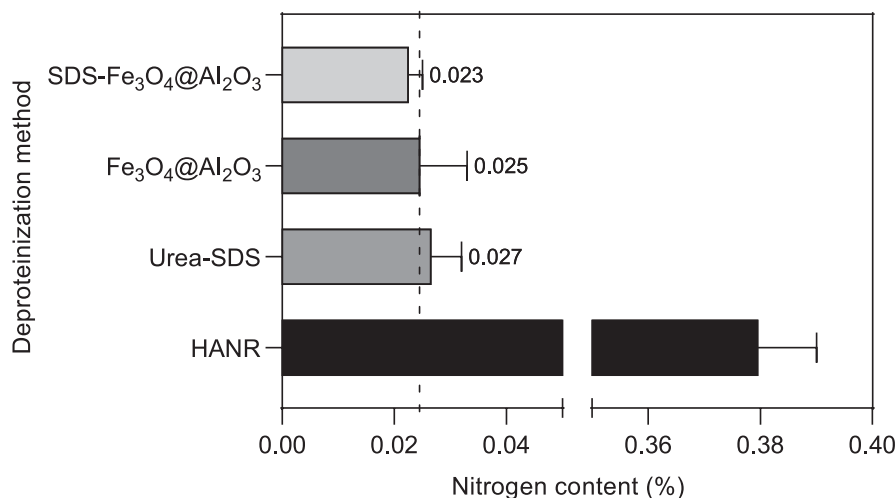


Figure 4. Nitrogen content of the obtained DPNR from various deproteinization (urea-SDS method using 0.10 wt.% urea and 3 batches of SDS, i.e., 1.00, 0.50, and 0.20 wt.%; $\text{Fe}_3\text{O}_4@\text{Al}_2\text{O}_3$ method using 1.00 wt.% $\text{Fe}_3\text{O}_4@\text{Al}_2\text{O}_3$; and SDS- $\text{Fe}_3\text{O}_4@\text{Al}_2\text{O}_3$ method using 0.10 wt.% SDS and 1.00 wt.% $\text{Fe}_3\text{O}_4@\text{Al}_2\text{O}_3$).

The properties of deproteinized natural rubber (DPNR) treated using $\text{Fe}_3\text{O}_4@\text{Al}_2\text{O}_3$

The utilization of $\text{Fe}_3\text{O}_4@\text{Al}_2\text{O}_3$ as protein removal from HANR was compared to deproteinization method that uses urea-SDS, and SDS- $\text{Fe}_3\text{O}_4@\text{Al}_2\text{O}_3$. The nitrogen content (N, in percentage) of the obtained deproteinized natural rubber (DPNR) that was prepared using those methods can be seen in Figure 4.

All DPNR that was prepared using various deproteinization showed a significant decrease in nitrogen content within the range of 0.023-0.027% compared to the nitrogen content of HANR (0.38%). Similar result was found on deproteinization using $\text{Fe}_3\text{O}_4@\text{Al}_2\text{O}_3$ and SDS- $\text{Fe}_3\text{O}_4@\text{Al}_2\text{O}_3$, 0.025 and 0.023%, respectively. This value showed insignificant result of $\text{Fe}_3\text{O}_4@\text{Al}_2\text{O}_3$ nanoparticle to reduce protein amount from HANR compared to urea-SDS. In other words, our result is quite interesting, though the different nitrogen content of DPNR is insignificant from those methods. Moreover, the use of $\text{Fe}_3\text{O}_4@\text{Al}_2\text{O}_3$ is a promising method characterized by its efficiency and simplicity. In the deproteinized HANR using nanoparticle, the incubation time is relative short, about 15-30 min, and the deproteinization can be performed as a continuous system. In the deproteinized HANR using urea-SDS, the incubation time was more than 60 min and should be prepared using batches system.⁵

The impact of dry rubber content to the nitrogen content in deproteinized HANR using method of SDS- $\text{Fe}_3\text{O}_4@\text{Al}_2\text{O}_3$ nanoparticle in the presence of SDS is shown in Figure 5. It shows the trend in reducing the ability of SDS- $\text{Fe}_3\text{O}_4@\text{Al}_2\text{O}_3$ when the dry rubber content of HANR was increased. The inability of $\text{Fe}_3\text{O}_4@\text{Al}_2\text{O}_3$ nanoparticle to bind the protein was due to the lack of nanoparticle loading in the

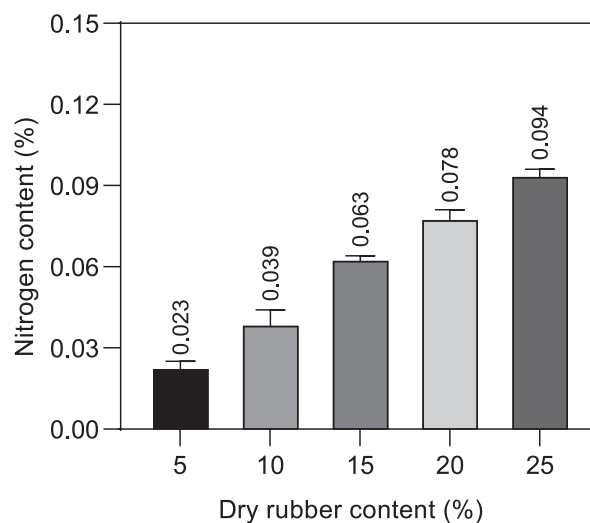


Figure 5. Nitrogen content of the obtained DPNR from various dry rubber content of HANR treated using $\text{Fe}_3\text{O}_4@\text{Al}_2\text{O}_3$ ($\text{Fe}_3\text{O}_4@\text{Al}_2\text{O}_3$ nanoparticle = 1.00 wt.%; SDS = 0.1 wt.%; incubation time = 30 min; pH = 11).

system. The nanoparticle of $\text{Fe}_3\text{O}_4@\text{Al}_2\text{O}_3$ was constructed by Al_2O_3 as shell, and Fe_3O_4 at core of nanoparticle. The role of Fe_3O_4 in this nanoparticle is to bring the magnetic property for improving the separation to be effective and efficient. On other hand, Al_2O_3 plays an important role as adsorbent to interact with the unwanted material (i.e., protein) due to its position in the outer shell. The interaction that occurred between Al_2O_3 and protein in HANR can be assumed as the physicochemical interaction of adsorption.^{18,19,23}

As mentioned previously, the protein removal treatment was performed at pH 11. The Al_2O_3 has been known as an amphoteric material that can have positive or negative charge on its surface depending on the pH of the system. Above pH 9.0 the Al_2O_3 will have negative net surface

charge due to the deprotonation of the surface of Al_2O_3 to form Al-O^- species. Normally, Al_2O_3 will interact with the organic molecules through electrostatic interaction when the pH of the system is below 9.0. At this current system, the negative charge of Al-O^- species will lead to the electrostatic repulsion between the Al-O^- species and negative charge of protein in HANR and it will affect the adsorption capacity to be much lower. In the conjunction with the presence of SDS in the system, SDS can interact with the Al_2O_3 surface and protein through hydrophobic interaction.²⁴ The hydrophobic interaction of SDS can be explained as the interaction of carbon chain of dodecyl with the carbon backbone of protein. The interaction of protein in the HANR with the surface of Al_2O_3 also can be explained as the hydrophobic interaction.²⁵⁻²⁷ The presence of SDS and protein in the system may induce a competitive or synergic hydrophobic interaction of those molecules to the surface of Al_2O_3 . However, the perfect way to discuss the real interaction between protein and the surface of adsorbent is still a big question. Within the current system, it can be assumed that the electrostatic interaction was not become a dominant interaction due to the similar charge of Al_2O_3 and the protein.²⁵ The interaction that happened among SDS, Al_2O_3 surface, and protein can be assumed to be dominated by hydrophobic interaction, and only small fraction will have electrostatic interaction, in case there is protein which has positive charge at pH 11.

Through the hydrophobic interaction and little fraction of electrostatic interaction, the interaction between Al_2O_3 surface and protein in HANR can be assumed as a multilayer formation. At the first step, the surface of Al_2O_3 particle will get masked by the protein. In the previous study²⁷ this phenomenon was confirmed through the zeta

potential value of Al_2O_3 . In the second step, the protein that attached on the surface of Al_2O_3 could interact with other free protein through electrostatic interaction, hydrogen bonding, van der Waals, and etc.

The utilization of high SDS concentration had been proven to reduce the nitrogen content significant, which was about 68.42% from 0.05 to 0.25 wt.% of SDS (Figure 6). The positive result of the SDS loading impact in the reduction of nitrogen content can be used as a basis for not increasing the amount of $\text{Fe}_3\text{O}_4@/\text{Al}_2\text{O}_3$ nanoparticle.

The contact time is one of important factors that influences the effectiveness of adsorbent to adsorb the adsorbate. In the current study, we have evaluated the impact of contact time, referred as incubation time, the ability $\text{Fe}_3\text{O}_4@/\text{Al}_2\text{O}_3$ nanoparticle method in the presence of SDS for removing protein. Figure 7 showed the correlation between incubation time and nitrogen content. The nitrogen content of processed HANR with various incubation times (15-75 min) showed fluctuate results (0.023-0.065%), yet not quite significant. From the Figure 7 it can be seen, that when the incubation time was only 30 min, the nitrogen content of the processed HANR can achieve a lower value, about 0.023%. Within the short incubation time and the effective result obtained during the process, it can be concluded that the optimum incubation time was 30 min. The fluctuate results in this study can be achieved due to low interaction between $\text{Fe}_3\text{O}_4@/\text{Al}_2\text{O}_3$ nanoparticle and protein present in the HANR. At the shorter contact time, the nitrogen content has a quite lower value due to the high ability of vacant adsorption site on the surface of $\text{Fe}_3\text{O}_4@/\text{Al}_2\text{O}_3$ nanoparticle. However, at the longer contact time, it can be assumed the adsorbed protein on the surface of $\text{Fe}_3\text{O}_4@/\text{Al}_2\text{O}_3$ nanoparticle can detach and interact with

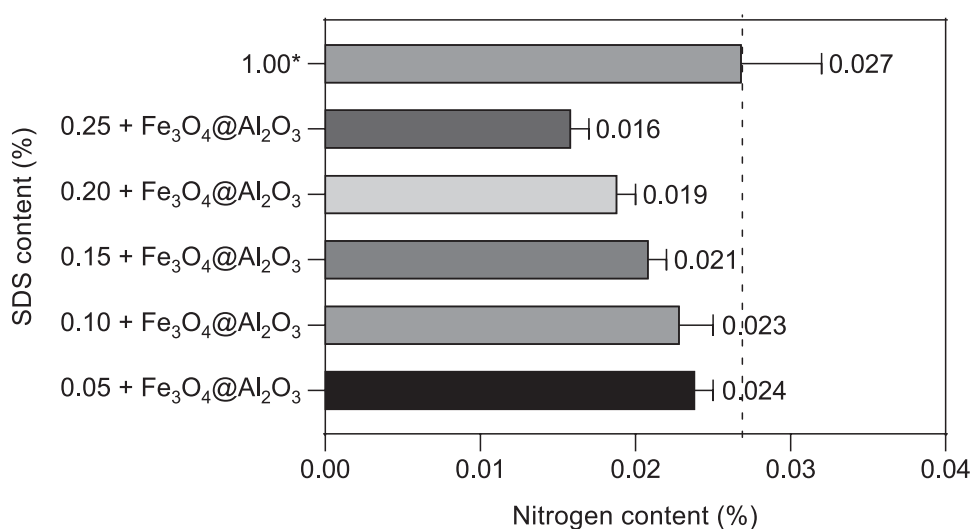


Figure 6. Nitrogen content of the obtained DPNR with various concentration of SDS ($\text{Fe}_3\text{O}_4@/\text{Al}_2\text{O}_3 = 1.00$ wt.%; dry rubber content = 10.00%; incubation time = 30 min; pH = 11). *In the presence of 0.1 wt.% urea and the addition of two other batches of SDS (0.50 and 0.20 wt.%).

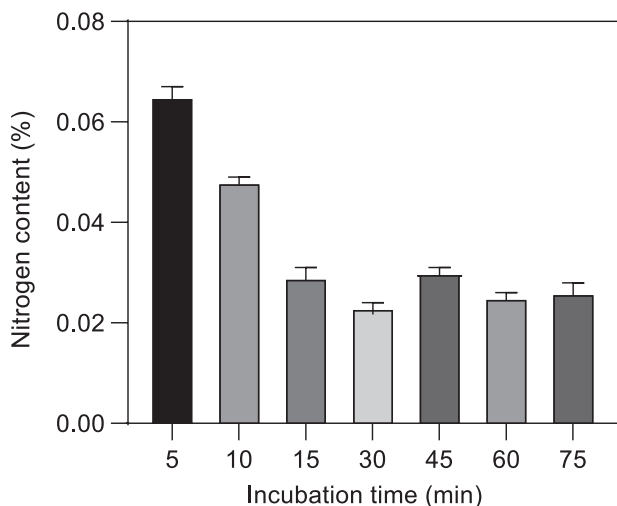


Figure 7. Nitrogen content of the obtained DPNR with various incubation time ($\text{Fe}_3\text{O}_4@Al_2O_3$ nanoparticle = 1.00 wt.%; dry rubber content = 10.00%; SDS = 0.10 wt.%; pH = 11).

the unbind proteins. These interactions cause the remaining active site on the surface of $\text{Fe}_3\text{O}_4@Al_2O_3$ nanoparticle hard to access.

Figure 8 showed the attenuated total reflection infrared (ATR IR) spectra of HANR and DPNR treated with SDS- $\text{Fe}_3\text{O}_4@Al_2O_3$ nanoparticle. NH stretching region of HANR showed a clear band at $3654-3191\text{ cm}^{-1}$. This band can be identified as the presence of proteins or long-chain peptides.⁵ After the treatment using $\text{Fe}_3\text{O}_4@Al_2O_3$ nanoparticle, the NH stretching band disappeared. However, in the previous study^{4,5} using urea-SDS treatment, a small band appeared at 3318 cm^{-1} , indicating as mono- or di-peptides. This result is a supporting evidence for claiming that the treatment using $\text{Fe}_3\text{O}_4@Al_2O_3$ nanoparticle can produce a lower protein natural rubber than urea-SDS treatment.

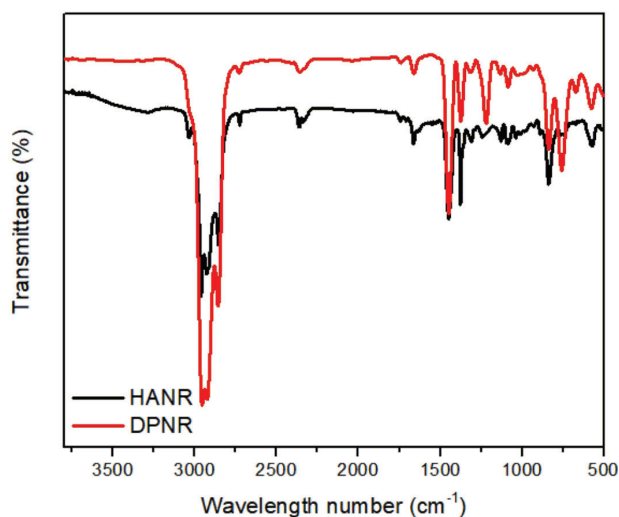


Figure 8. ATR IR spectra of HANR and DPNR.

Figure 9 shows the glass transition temperature (T_g) of DPNR and HANR treated with SDS- $\text{Fe}_3\text{O}_4@Al_2O_3$ nanoparticle in the presence of SDS. The T_g value of HANR increased few degrees after deproteinized using SDS- $\text{Fe}_3\text{O}_4@Al_2O_3$ nanoparticle. This result was also found in the previous study conducted by Klinklai *et al.*³⁶ This anomaly occurred due to the suppression of micro-Brownian motion, the presence of network formation is indicated as the main reason of this phenomenon, especially due to the presence of branched-chain protein and fatty acid that still remain in the HANR treated by SDS- $\text{Fe}_3\text{O}_4@Al_2O_3$.^{9,36} Further study needs to investigate the correlation of $\text{Fe}_3\text{O}_4@Al_2O_3$ nanoparticle loading content with the percentage of N content of the resulting DPNR since the use of $\text{Fe}_3\text{O}_4@Al_2O_3$ nanoparticle in the physical adsorption or immobilization protein showed a possibility to be developed as an advanced method due to its effectiveness and efficiency.

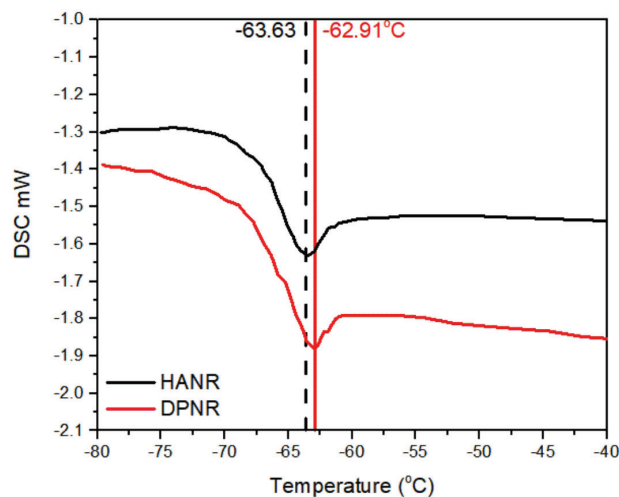


Figure 9. Differential scanning calorimetry (DSC) curve of HANR and DPNR.

Conclusions

The as-prepared $\text{Fe}_3\text{O}_4@Al_2O_3$ nanoparticle that had irregular shaped and particle size of 16-28 nm was able to remove protein from HANR solution. Kjeldahl method proved that the utilization of $\text{Fe}_3\text{O}_4@Al_2O_3$ could reduce the protein content from 0.38 to 0.016% in an optimum condition (dry rubber content 10.00%; 0.25% surfactant; 1.00 wt.% $\text{Fe}_3\text{O}_4@Al_2O_3$; and 15 min of incubation time). The protein removal process using SDS- $\text{Fe}_3\text{O}_4@Al_2O_3$ nanoparticle showed an insignificant result compared to deproteinization method using urea-SDS. However, this method offered a more effective, efficient in time and simpler procedure than the previous one (urea-SDS), yet it can be done in a continuous process. The presence of

coated magnetic material and SDS plays significance role during the protein removal process through anionic-cationic and hydrophobic-hydrophobic interaction. Through these advantages, this method has a great opportunity to be developed and applied in the future.

Acknowledgments

This research was funded by Vietnam National Foundation for Science and Technology Development (NAFOSTED) under grant No. 104.02-2016.47.

Author Contributions

I. P. Mahendra was responsible for investigation, visualization, writing original draft; Mai K. Linh for investigation, writing original draft; Nguyen N. Thang for data curation, validation; Vu T. Thuy for data curation, validation; Le T. Trang for investigation; Le X. Think for investigation; Nguyen T. H. Phuong for validation, visualization; Nguyen T. Ha for validation, writing original draft; Nghiem T. Thuong for validation, data curation; Seiichi Kawahara for writing-review and editing; Yoshimasa Yamamoto for writing-review and editing; Phan T. Nghia for conceptualization, formal analysis funding acquisition, writing-review and editing.

References

- Perrella, F. W.; Gaspari, A. A.; *Methods* **2002**, *27*, 77.
- Nanti, S.; Wongputtisin, P.; Sakulsingharoj, C.; Klongklaew, A.; Chomsri, N.; *Food Appl. Biosci. J.* **2014**, *2*, 216.
- Pichayakorn, W.; Suksaeree, J.; Taweepreda, W.; *Adv. Mater. Res.* **2014**, *844*, 474.
- Yamamoto, Y.; Nghia, P. T.; Klinklai, W.; Saito, T.; Kawahara, S.; *J. Appl. Polym. Sci.* **2008**, *107*, 2329.
- Kawahara, S.; Klinklai, W.; Kuroda, H.; Isono, Y.; *Polym. Adv. Technol.* **2004**, *15*, 181.
- Klinklai, W.; Saito, T.; Kawahara, S.; Tashiro, K.; Suzuki, Y.; Sakdapipanich, J. T.; Isono, Y.; *J. Appl. Polym. Sci.* **2004**, *93*, 555.
- Chaikumpollert, O.; Yamamoto, Y.; Suchiva, K.; Nghia, P. T.; Kawahara, S.; *Polym. Adv. Technol.* **2012**, *23*, 825.
- Wongputtisin, P.; Khanongnuch, C.; Khongbantad, W.; Niamsup, P.; Lumyong, S.; *J. Appl. Microbiol.* **2012**, *113*, 798.
- Kawahara, S.; Kakubo, T.; Suzuki, M.; Tanaka, Y.; *Rubber Chem. Technol.* **1999**, *72*, 174.
- Nun-anan, P.; Wisunthorn, S.; Pichaiyut, S.; Nathaworn, C. D.; Nakason, C.; *Polym. Adv. Technol.* **2019**, *31*, 44.
- Nun-anan, P.; Wisunthorn, S.; Pichaiyut, S.; Vennemann, N.; Kummerlöwe, C.; Nakason, C.; *Polym. Test.* **2020**, *89*, 106623.
- Beezhold, D. H.; Owego, N. Y.; *US pat. 5563241A*, **1996**.
- Mohseni-Bandpi, A.; Kakavandi, B.; Kalantary, R. R.; Azari, A.; Keramati, A.; *RSC Adv.* **2015**, *5*, 73279.
- Kakavandi, B.; Takdastan, A.; Jaafarzadeh, N.; Azizi, M.; Mirzaei, A.; Azari, A.; *J. Photochem. Photobiol., A* **2016**, *314*, 178.
- Azari, A.; Kalantary, R. R.; Ghanizadeh, G.; Kakavandi, B.; Farzadkia, M.; Ahmadi, E.; *RSC Adv.* **2015**, *5*, 87377.
- Adlnasab, L.; Shekari, N.; Maghsodi, A.; *J. Environ. Chem. Eng.* **2019**, *7*, 102974.
- Chen, C. T.; Chen, Y. C.; *J. Biomed. Nanotechnol.* **2008**, *4*, 73.
- Li, Y.; Liu, Y.; Tang, J.; Lin, H.; Yao, N.; Shen, X.; Deng, C.; Yang, P.; Zhang, X.; *J. Chromatogr. A* **2007**, *1172*, 57.
- Peng, H. P.; Liang, R. P.; Qiu, J. D.; *Biosens. Bioelectron.* **2011**, *26*, 3005.
- Tekiye, E. S.; Aghajani, Z.; Sharif, M. A.; *J. Mater. Sci.: Mater. Electron.* **2017**, *28*, 5360.
- Xiang, G.; Li, L.; Jiang, X.; He, L.; Fan, L.; *Anal. Lett.* **2013**, *46*, 706.
- Liu, J.-c.; Tsai, P.-j.; Lee, Y. C.; Chen, Y.-c.; *Anal. Chem.* **2008**, *80*, 5425.
- Mohamed, S. A.; Al-Harbi, M. H.; Almulaiky, Y. Q.; Ibrahim, I. H.; El-Shishtawy, R. M.; *Electron. J. Biotechnol.* **2017**, *27*, 84.
- Nguyen, T. M. T.; Do, T. P. T.; Hoang, T. S.; Nguyen, N. V.; Pham, H. D.; Nguyen, T. D.; Pham, T. N. M.; Le, T. S.; Pham, T. D.; *Int. J. Polym. Sci.* **2018**, *2018*, 2830286.
- Puddu, V.; Perry, C. C.; *ACS Nano* **2012**, *6*, 6356.
- Chen, W. Y.; Huang, H. M.; Lin, C. C.; Lin, F. Y.; Chan, Y. C.; *Langmuir* **2003**, *19*, 9395.
- Rezwan, K.; Meier, L. P.; Rezwan, M.; Voros, J.; Textor, M.; Gauckler, L. J.; *Langmuir* **2004**, *20*, 10055.
- Chen, H.; Shi, X. H.; Zhu, Y. F.; Zhang, Y.; Xu, J. R.; *J. Appl. Polym. Sci.* **2008**, *107*, 3049.
- Hanan, F. H. Ab.; Yusof, Y. M.; Resali, N. S. M.; Dasril, R. S. D.; Azman, N. S.; Zawawi, A. H. S.; Hussein, H. I.; Rahim, K. A.; Kassim, N. M.; Rizuan, M. I. R.; *RRIM Test Methods for Standard Malaysian Rubbers SMR Bulletin No. 7 (revised edition)*, Part B.5; Malaysian Rubber Board: Malaysia, 2018.
- Schindelin, J.; Arganda-Carreras, I.; Frise, E.; Kaynig, V.; Longair, M.; Pietzsch, T.; Preibisch, S.; Rueden, C.; Saalfeld, S.; Schmid, B.; Tinevez, J.-Y.; White, D. J.; Hartenstein, V.; Eliceiri, K.; Tomancak, P.; Cardona, A.; *Nat. Methods* **2012**, *9*, 676.
- Jung, K. W.; Choi, B. H.; Ahn, K. H.; Lee, S. H.; *Appl. Surf. Sci.* **2017**, *423*, 383.
- Bristy, S. S.; Rahman, M. A.; Tauer, K.; Minami, H.; Ahmad, H.; *Ceram. Int.* **2018**, *44*, 3951.
- Iconaru, S. L.; Guégan, R.; Popa, C. L.; Motelica-Heino, M.; Ciobanu, C. S.; Predoi, D.; *Appl. Clay Sci.* **2016**, *134*, 128.

34. Potdar, H. S.; Jun, K.-W.; Bae, J. W.; Kim, S.-M.; Lee, Y.-J.; *Appl. Catal., A* **2007**, *321*, 109.
35. Zhang, J.; Guo, Q.; Liu, Y.; Cheng, Y.; *Ind. Eng. Chem. Res.* **2012**, *51*, 12773.
36. Klinklai, W.; Kawahara, S.; Mizumo, T.; Yoshizawa, M.; Tangpakdee Sakdapipanich, J.; Isono, Y.; Ohno, H.; *Eur. Polym. J.* **2003**, *39*, 1707.

Submitted: January 29, 2020

Published online: September 9, 2020

